



## Research Article

# Assessment of cytotoxic features of corn oil-derived carbon nanostructures decorated palmitic acid

Abdullah Almubarak<sup>a</sup>, Vaiyapuri Subbarayan Periasamy<sup>a</sup>, Jegan Athinarayanan<sup>a</sup>, Ali A Alshatwi<sup>a,\*</sup>

<sup>a</sup>Department of Food Science and Nutrition, King Saud University, College of Food Science and Agriculture, Riyadh, 11451, Saudi Arabia

## ARTICLE INFO

**Keywords:**  
Carbon nanostructures  
Cytotoxicity  
Edible oil  
THP-1 cells

## ABSTRACT

Carbon based materials has garnered significant attention because of their potential biomedical applications and environmental implications. In this present study, we synthesized carbon nanostructures (CNs) using corn oil as a precursor through a flame synthesis approach and investigates the cytotoxic impact of CNs on Tohoku Hospital Pediatrics-1 (THP-1) macrophages. The synthesized CNs elemental composition, functional groups, morphology, and crystalline characteristics were studied by adopting different techniques, including X-ray photoelectron spectroscopy, Fourier transform infrared spectroscopy (FTIR), transmission electron microscopy (TEM), and X-ray diffractometry (XRD). The TEM images confirms 70 – 100 nm with spherical CNs were synthesized from corn oil. The XPS spectrum of corn oil-derived carbon nanostructures (CCNs) exhibits distinct atomic peaks of C1s and O1s at 284.2 and 532.8 eV. The CCNs surface were decorated with palmitic acid (PA) and impact on cell viability and morphology was investigated through 3-(4,5-dimethylthiazol-2-yl)-2,5-diphenyltetrazolium bromide (MTT) assay and acridine orange/ethidium bromide (AO/EB) staining in THP-1 derived macrophages. The CCNs/PA were do not promote cell death and morphological features in macrophages. Our *in vitro* cytotoxicity assessment revealed that CCNs/PA displayed good compatibility. Overall, our study contributes crucial insights into the biological impact of CCNs/PA and underscores the need for careful assessment of their biomedical applications.

## 1. Introduction

Carbon-based nanostructures have received significant interest in recent years due to their extraordinary electrical, catalytic, and optical features (Gusain *et al.*, 2020; Riley and Narayan, 2021). Recently, several studies have reported the preparation of carbon-based nanostructures such as carbon nanofibers, carbon nanotubes, graphene oxide, reduced graphene oxide, graphene, carbon quantum dots, graphitic carbon nitride, fullerenes, carbon nano-onions, and carbon nanosheets (Gusain *et al.*, 2020; Clancy *et al.*, 2018). Carbon-based nanostructures have been exploited in various applications such as bio-sensors, bio-imaging, supercapacitors, solar cells, fuel cells, cancer therapy, adsorbents, catalysts, photovoltaic cells, and drug delivery (Bagheri *et al.*, 2022; Georgakilas *et al.*, 2015; Feng *et al.*, 2024; Kaare *et al.*, 2024; Yang *et al.*, 2023; Malode *et al.*, 2024). Carbon-based materials generally contain hybridized sp<sup>2</sup> carbon, except nanodiamonds, possessing hybridized sp<sup>3</sup> carbon. However, carbon-based nanostructures exhibit fascinating physical and chemical characteristics. Due to their complex synthesis processes, they are limited to small-scale usages and laboratories (Mulay *et al.*, 2019; Singh *et al.*, 2025). As a result of partial pyrolysis/combustion, soot carbon is derived from organic substances. As a result of combustion, soot carbon is defined as waste. Earlier studies have exploited various methods to synthesize carbon nanostructures, such as

sonication, hydrothermal, microwave, carbonization, chemical vapor deposition, and chemical oxidation approaches (Athinarayanan *et al.*, 2020b; Zhu *et al.*, 2009; Alsaffar *et al.*, 2023; Arroyo-Arroyo *et al.*, 2024; Shen *et al.*, 2013). These techniques have some draw-backs, including hazardous chemical usage, high costs, and poor yield. Currently, carbon nanostructures (CNs) are synthesized from different sustainable, cost-effective, renewable, and environmentally friendly substances. Edible oils with high carbon atom contents are ideal materials for synthesizing CNs. For example, various seed oils, including pumpkin, fenugreek, poppy, watermelon, and funnel oil, have been exploited to produce CNs (Nadeem *et al.*, 2024). In fact, turning carbon soot into CNs is a sustainable approach to reducing the harmful impacts of soot particles. CNs are zero-dimensional materials with a 1 - 100 nm range, and they have a wide range of potential applications in various fields due to their unique properties, including electrical, optical, thermal, mechanical, and biological features (Nadeem *et al.*, 2024; Ramar and Balraj, 2022; Saini *et al.*, 2021).

The monocytes and macrophages are vital components of the innate immune re-sponse, including antigen presentation, phagocytosis, and pro- and anti-inflammatory cytokine secretion (Germic *et al.*, 2019). During inflammatory conditions, macrophages arise from monocytes (Yan and Hansson, 2007). Consequently, macrophages can respond to various external stimuli, including microbe- or damage-associated

### \*Corresponding author:

E-mail address: nano.alshatwi@gmail.com alshatwi@ksu.edu.sa (A A Alshatwi)

Received: November, 2025 Accepted: January, 2026 Epub Ahead of Print: 06 May, 2026 Published: \*\*\*

DOI: 10.25259/JKSUS\_1824\_2025

molecular patterns, which affect macrophage activation state and morphology (Shapouri-Moghaddam et al., 2018). The THP-1 cell line originated from human leukemia and has been extensively used to examine the immune response potential of monocytes and monocyte-derived macrophages, owing to the resemblance of their activity to human peripheral blood mononuclear cells (Qin, 2012). In THP-1 macrophages, carboxylated and hydroxylated MWCNTs triggered interleukin-8 secretion and lipid accumulation (Long et al., 2019). Kinaret et al. study suggested that carbon-based materials induced time- and dose-dependent induction of IL-1 $\beta$ , tumor necrosis factor, IL-10, and CSF1 gene expression in THP-1-derived macrophages (Kinaret et al., 2020). Interestingly, carbon black nanoparticles triggered reactive oxygen species (ROS) levels and enhanced the lipid accumulation in THP-1-derived macrophages (Cao et al., 2014). Macrophages and lymphocytes play a crucial role in immune defense, and any adverse effects on these cells could lead to immune dysfunction. According to previous studies, carbon-based materials promote immunotoxicity. Palmitic acid (PA) is a widely distributed saturated fatty acid in blood plasma. It is prevalent in palm oil, cocoa butter, olive oil, meat, and dairy products. According to data, the average intake of PA is between 20 and 30 grams/day (Carta et al., 2017). Earlier studies reported that PA modulates the differentiation of M1 macrophages (Korbecki and Bajdak-Rusinek, 2019). According to the Erbay et al., (2009) study, PA exposure stimulates macrophage inflammatory activity by upregulating fatty acid-binding protein 4. Also, Rosa Neto et al., (2021) study demonstrated that PA can provoke macrophages by activating the Toll-like receptor 4. The surface charge and hydrophobicity of corn oil-derived carbon nanostructures (CCNs) may be altered by PA, potentially impacting their interaction with macrophages and other immune cells. Nevertheless, the impact of PA-associated CCNs on THP-1-derived macrophages is unclear. Therefore, understanding the interaction of CCNs/PA with immune cells is essential for assessing their safety in biomedical applications. In this study aims to assess the cytotoxicity of PA-linked CCNs in THP-1-derived macrophages.

## 2. Materials and Methods

### 2.1 Materials

We have received PA from BDH Laboratories Supplies, UK. We have purchased phorbol 12-myristate 13-acetate (PMA) from MedChemExpress, USA. Acridine orange (AO), MTT dye, Giemsa stain, dimethyl sulfoxide (DMSO), and Ethidium bromide (EB) were received from Sigma-Aldrich (St. Louis, MO, USA). Fetal bovine serum and RPMI-1640 medium were obtained from Invitrogen (Carlsbad, California, USA).

### 2.2 CCNs synthesis

To synthesize the CCNs, about 25 mL of corn oil was poured into a clay pot. Cotton wicks were wholly immersed in oil except for the end tails. Then, the wick end tail was lighted, and the glass plate was kept above the fire. Afterward, the fire was permitted to burn continuously via the capillary action of the cotton wick. The carbon was applied to the glass surfaces. It was conducted in a fume hood to ensure the synthesis process was ventilated correctly. The resulting carbon was collected and dispersed in ethanol using ultrasonication at 750 W for 15 mins. Then, the carbon particles were washed with ethanol through centrifugation. The corn oil-derived CCNs were labeled as CCNs.

### 2.3 Fabrication of CCNs decorated PA

Approximately 20 mg of CCNs were mixed with 20 mg of PA. The mixture was boiled at 200°C for 30 min to promote the interaction of the PA and CCNs. Afterward, the obtained samples were washed with ethanol using centrifugation for further analysis.

### 2.4 Analysis of carbon nanostructures

We investigated the surface composition of CCNs using X-ray photoelectron spectroscopy (XPS); it was conducted on the ESCA1600 system (ULVAC-PHI Inc., Tokyo, Japan) using an Al K-alpha X-ray source and a hemispheric electron analyzer. A transmission electron microscopy (TEM) was used to examine the structural features of the CCNs at an accelerating potential of 120 kV. The CCNs were dispersed in ethanol using ultrasonication and dropped on a carbon-coated copper grid for TEM observation. Fourier transform infrared spectroscopy (FTIR) was carried out by FT/IR-6300 with ATR PRO610P-S (JASCO). We obtained the carbon nanoparticle's X-ray diffraction pattern using a RINT ULTIMA X-ray diffractometry (XRD) system (Rigaku Co., Tokyo, Japan) with a Ni filter and a Cu-K $\alpha$  source. The prepared samples were dispersed in distilled water using ultrasonication, and the hydrodynamic size of CCNs analyses were performed on Malvern Zetasizer nanoserries, Nano-ZS90 (Malvern Inst. Ltd, Malvern, UK).

### 2.5 Cell culture

Human leukemia THP-1 cells were purchased from the American type culture collection (ATCC), USA. To maintain THP-1 cells, we used RPMI-1640 medium supplemented with antibiotics (100 U/ml penicillin and 100  $\mu$ g/ml streptomycin) and 10% fetal bovine serum. Incubation was performed at 37°C under 5% carbon dioxide. The THP-1 cells were differentiated into macrophages using 10 ng/mL PMA overnight exposure for cytotoxicity assessment experiments (Phuangbubpha et al., 2023). It was observed that THP-1-derived macrophages adhered to the surfaces of the cell culture plates.

### 2.6 Analysis of cell viability

The impact of CCNs and CCNs/PA on the cell viability of THP-1-derived macrophages was investigated using MTT assay (Athinarayanan et al., 2024; 2025). The macrophages were cultured into 96-well plates. The CCNs and CCNs/PA were dispersed in RPMI-1640 media using ultrasonication. Afterwards, the CCNs and CCNs/PA were exposed to macrophages with different concentrations, including 0, 25, 50, 100, 200, and 400  $\mu$ g/mL for 24 and 48 h. Then, the MTT dye was added to each well and kept for 6 h in the dark at 37°C. Then, the cell survival rate was determined by measuring the O.D. value of each well. Each experiment was performed three times separately.

### 2.7 AO/EB assay

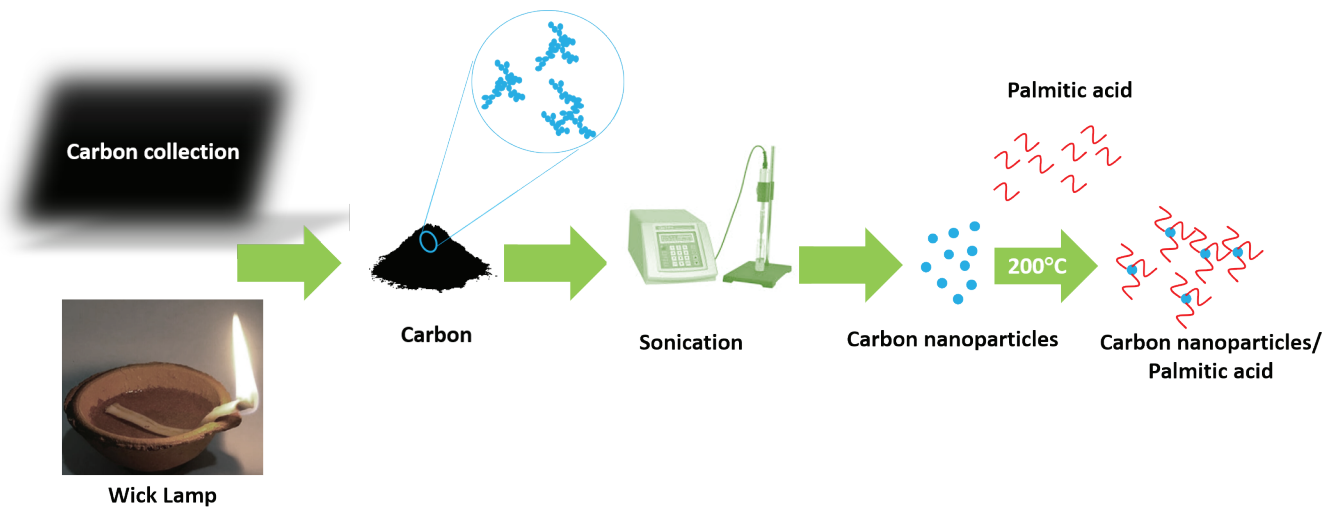
About  $1 \times 10^5$  macrophage cells were cultured in 24-well plates and exposed to CCNs and CCNs/PA for 24 h. After exposure, the macrophage cells morphological features were examined using bright-field microscopy (Habelreth et al., 2025). For fluorescent microscopy analysis, cells were stained with AO/EB dual stain for 2 min at 37°C (Athinarayanan et al., 2018). The stained control and treated cells were examined under fluorescence microscopy.

### 2.8 Giemsa staining assay

Briefly,  $1 \times 10^5$  macrophage cells were cultured in 24-well plates and exposed to CCNs for 24 h. According to the manufacturer's instructions, the cells were fixed with formaldehyde for 15 min at 37°C. Next, the cells were washed with phosphate buffer saline and stained with Giemsa for 10 min at room temperature. The stained cells were examined under an optical microscope. Generally, apoptotic cells were shown in blue, and normal or necrotic cells were darker.

### 2.9 Oil red O staining

The Oil Red O staining assay was carried out to identify the fatty acid accumulation. The macrophages were cultured in 24-well plates and treated with CCNs-PA for 24 h. Afterward, cells were fixed for 30 min and stained with Oil Red O stain at 37°C for 60 mins. The cells were washed thrice with PBS, and cells were examined and imaged.



Scheme 1. Schematic representation of the fabrication of PA decorated CCNs.

### 2.10 Statistical analysis

All statistical analysis was performed using Microsoft Excel Software. All the data are presented as the mean  $\pm$  SD.  $P$  value  $<$  0.05 was considered to be a statistically significant difference.

## 3. Results and Discussion

### 3.1 Synthesis and characterization of CCNs

An edible oil serves as a sustainable resource for carbon nanostructures. The edible oil is burned in cotton wicks' flame, producing carbon particles (Scheme 1). The aggregated carbon particles were dispersed under an ultrasonication process to achieve the formation of a carbon nanostructure. As similar, some studies synthesized carbon-based materials through wick-and-oil flame synthesis process. For example, Tyagi et al., (2022) study reported that mustard oil was exploited as sustainable resource for activated carbon preparation through wick-and-oil flame synthesis process. Periasamy et al., (2024) study suggested that carbon nano-onions have been synthesized using ghee as precursor. In addition, candle soot is used to prepare carbon nanoparticles (Kanakaraj and Sudakar, 2020). Scheme 1 represents the preparation of CCNs/PA. The CCNs surface was functionalized with PA

at 200°C. The PA melts and interacts with the surface functional groups of CCNs. The long hydrocarbon chains of PA orient outward, forming a hydrophobic coating around the CCNs.

Fig. 1 shows the FTIR spectra of CCNs and CCNs/PA. These results show different absorption peaks around 2158, 2000, and 1978  $\text{cm}^{-1}$ . The band around 2158  $\text{cm}^{-1}$  corresponds to the stretching vibrations of carbon-carbon ( $\text{C}=\text{C}$ ). In addition, the FTIR absorption band between 1900 - 2100  $\text{cm}^{-1}$  is associated with defective carbon nanoparticles. Also, these structures may form in amorphous or partially graphitized carbon materials. The synthesized CN's particle size distribution was measured using a particle size analyzer. The prepared CCNs average particle size is 179 nm (Fig. 2). In addition, we have analyzed average particle size distribution of CCNs/PA, results indicate that particle size of CCNs/PA is 196 nm (Fig. 2). An average particle size of prepared nanostructures is greater than that acquired from the TEM observation because of aggregation (Athinarayanan et al., 2022).

XPS is often used to characterize the chemical state of surfaces of carbon-based compounds. The XPS spectrum of the CCNs are represented in Fig. 3. The XPS scans displayed that CCNs possess 2 peaks, corresponding to C1s and O1s. We examined the strong signal of the C1s peak compared to the O1s peak, revealing that CCNs are predominantly carbon with minimal oxygen. These peaks originate from the valence electron relaxation of carbon atoms in response to

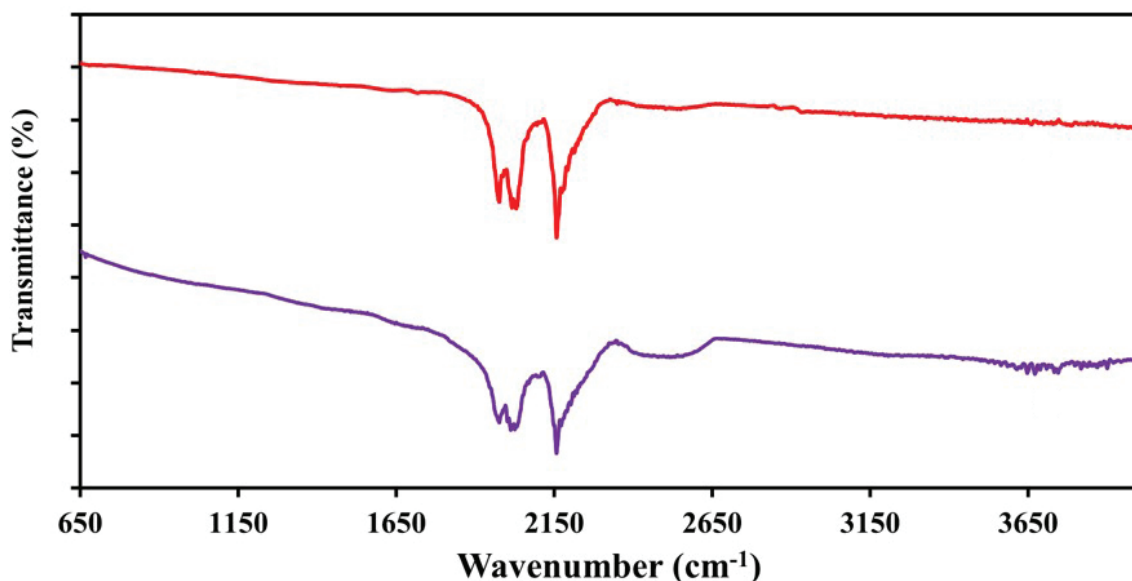


Fig. 1. FTIR spectra of (blue) CCNs and (red) CCNs/PA.

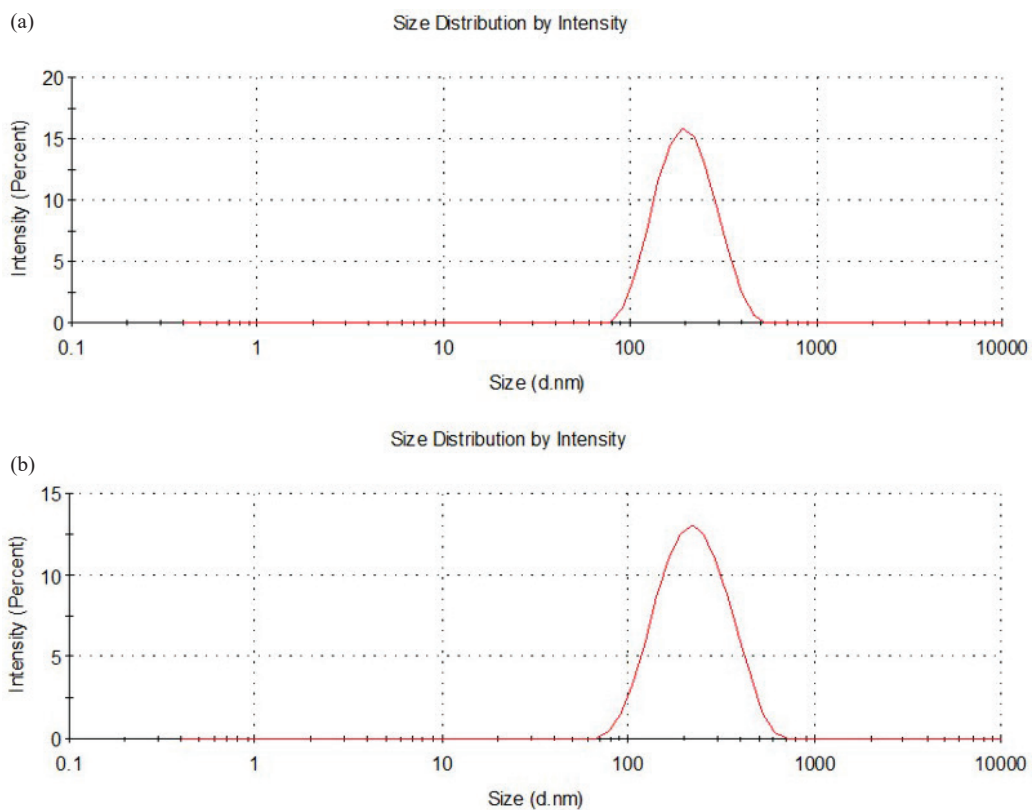


Fig. 2. Particle size distribution of (a) CCNs and (b) CCNs/PA. The prepared nanostructures were dispersed in distilled water and particle size distribution was determined using dynamic light scattering (DLS) approach.

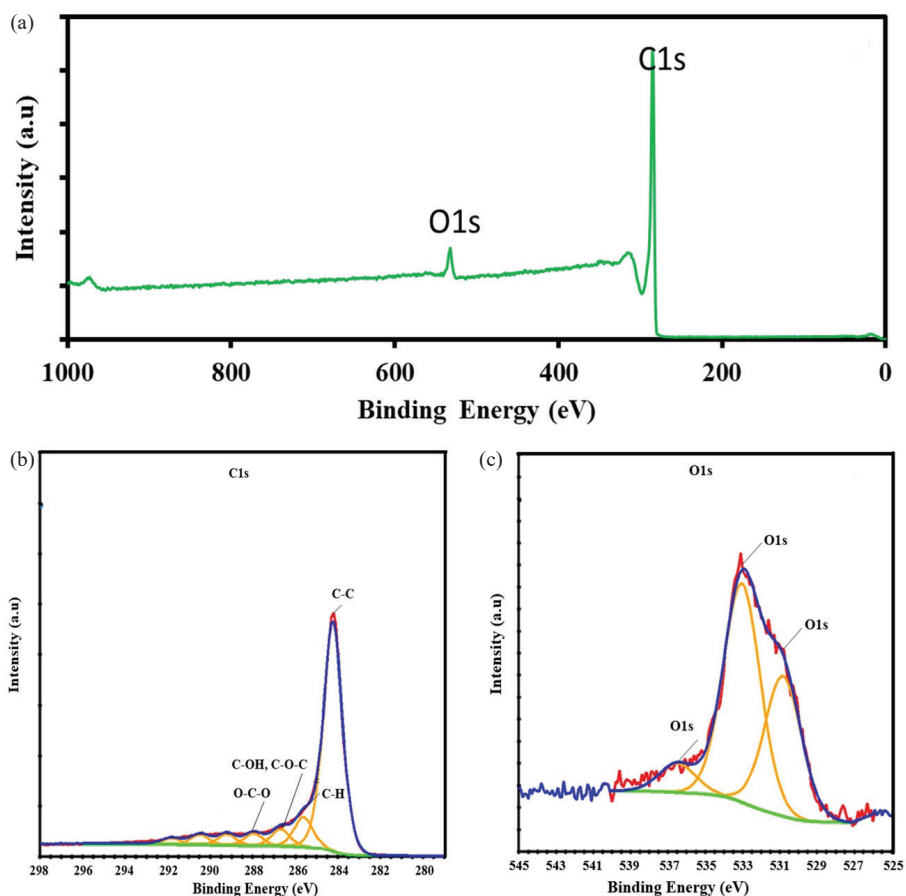


Fig. 3. X-ray photoelectron (a) survey spectra and high-resolution spectra of (b) C1s and (c) O1s of carbon nanostructures derived from corn oil.

their ejection due to photoionization generated by exposure to X-rays. According to the arrangement of carbon atoms, peak intensities and shapes vary. There are five peaks in the deconvolution of the C1s, i.e., a prominent peak at 284.2 eV associated with sp<sup>2</sup> hybrids C-C bonds, 285.5 eV assigned to sp<sup>3</sup> C-O, 286.5 eV related to C-sp<sup>3</sup>-OH, 287.8 denoting O-C-O, and 288.9 eV related to -C-sp<sup>2</sup> COOH- bond. Sp<sup>2</sup> hybridization of carbon is attributed to graphitic carbon, while sp<sup>3</sup> hybridization is associated with the amorphous carbon of CCNs. The O1s have three deconvolution peaks, i.e., C-O at 531.2 eV, C-O-H at 536.5 eV, and COOH at 533.3 eV. The surface of CCNs contains a band between carbon and oxygen.

In order to determine the crystalline properties of synthesized CCNs, XRD measurements were performed. XRD spectra of prepared nanostructures are shown in Fig. 4. There is a broad peak around  $2\theta = 24.3$ , which was identified as the (002) plane, assigned to the presence of large amounts of amorphous CNs connected with graphite hexagonal lattice. According to previous studies reported that peak indicates the existence of huge amount of amorphous material associated with CNs (Atchudan et al., 2020; Wang et al., 2022). We found that our study results

were consistent with previous studies (Atchudan et al., 2020; Wang et al., 2022). Transmission electron microscopic images of CCNs revealed that 70 – 100 nm in diameter spherical particles were associated with the formation of clusters (Fig. 5). According to TEM images, CNs form a fractal chained structure. Also, the CCNs TEM images are identical. Our TEM results are highly closed to earlier studies. For instance, Chang et al., (2021) study demonstrated that oil-derived carbon nanoparticles possess spherical shape with aggregate forms.

### 3.2 Cytotoxicity analysis of CCNs decorated PA

Macrophages were derived from human THP-1 cells through differentiation using PMA. Meanwhile, the suspension THP-1 cells changed into adherent macrophages. Macrophages are one of the essential components of the innate immune system. Macrophages involve phagocytosis and pro- and anti-inflammatory cytokine secretion during inflammatory conditions. We assessed the cytotoxicity of PA decorated CNs using THP-1 macrophages as an *in vitro* model. To investigate the impact of CCNs and CCNs/PA on cell viability and intracellular

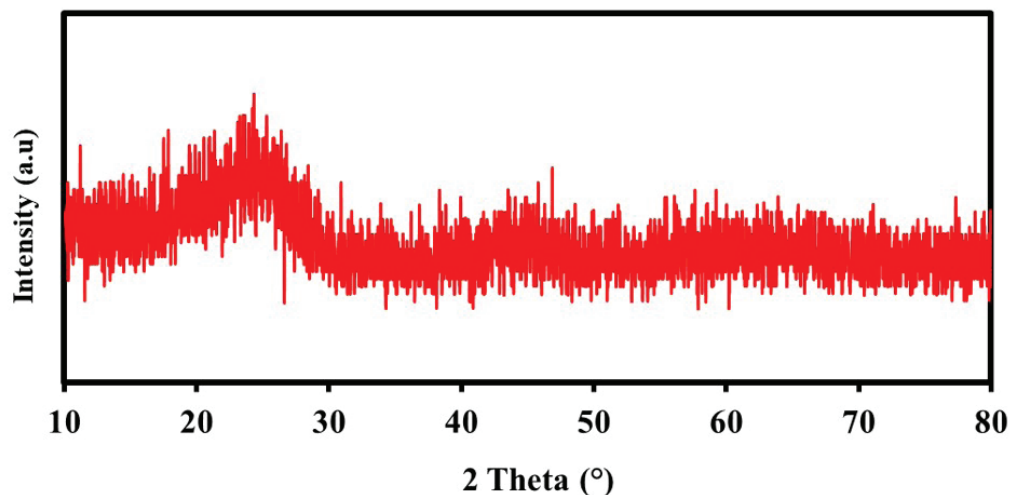


Fig. 4. X-ray diffraction pattern of carbon nanostructures derived from corn oil.

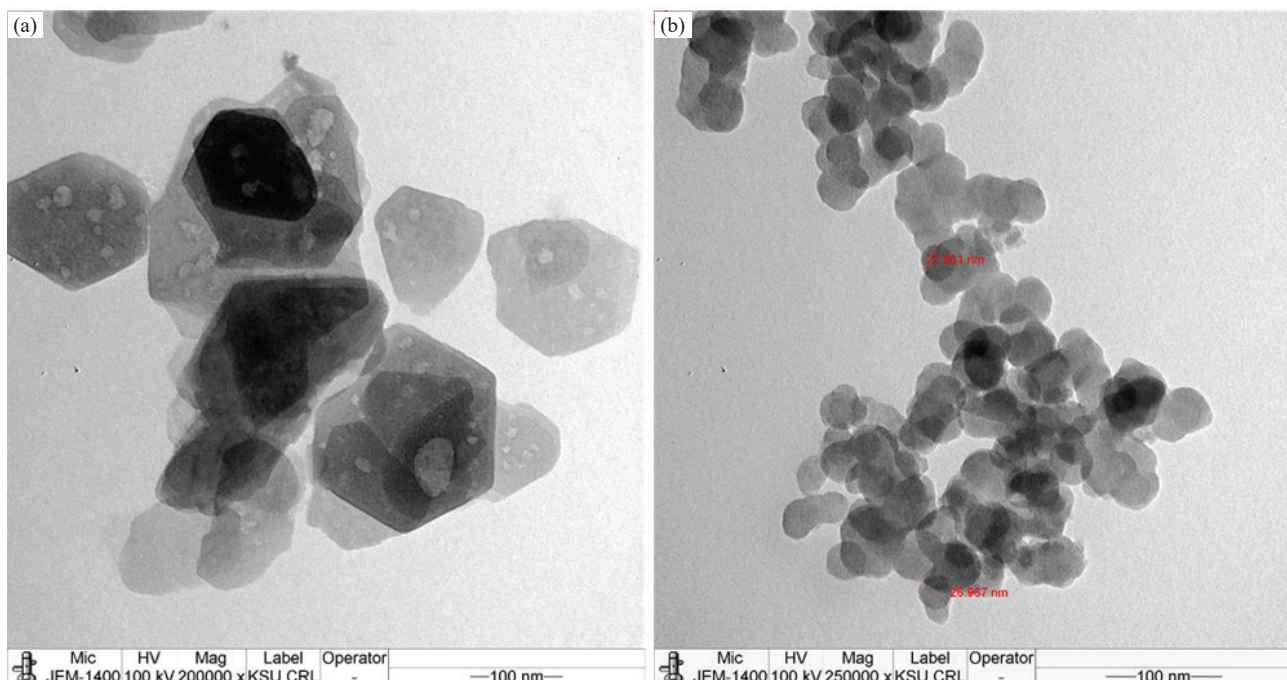
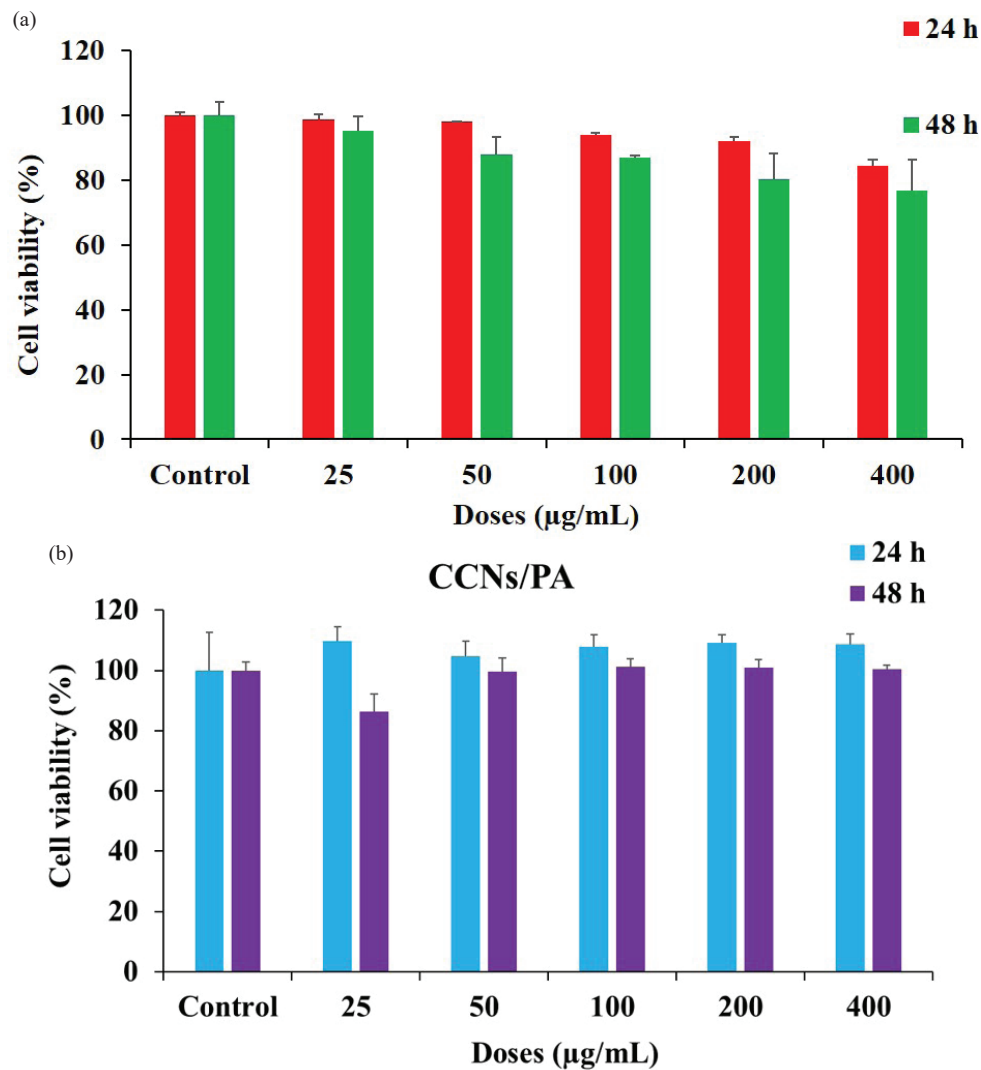


Fig. 5. (a-b) TEM images of carbon nanostructures derived from corn oil.



**Fig. 6.** (a) Cell viability evaluation of THP-1 macrophages after exposure to CCNs. All the represented data were collected from triplicates. (b) Cell viability evaluation of THP-1 macrophages after exposure to CCNs/PA. All the represented data were collected from triplicates. There was no significant difference among the groups ( $P > 0.05$ ).

uptake. Choosing the dose carefully when conducting experiments on nanoparticle cytotoxicity and cell uptake is important because extremely high dose levels cannot exhibit variable cellular uptake due to particle overload and/or cell death caused by nanoparticles. The prepared CCNs and CCNs/PA were dispersed in cell culture media using ultrasonication process for cytotoxicity assessment. According to our experiments with THP-1 macrophages, 50 and 100  $\mu\text{g/mL}$  was the dose at which differential cellular uptake occurred without macrophage cytotoxicity. Figs. 6(a) and (b) shows the effect of CCNs and CCNs/PA on the viability of THP-1 macrophages. We noticed that CCNs promotes cell viability reduction in macrophages by dose- and time-dependent manner.

In contrast, the cell viability slightly increased in the 25, 50, 100, 200, and 400  $\mu\text{g/mL}$  CCNs/PA exposure. The cell viability assay results revealed that CCNs/PA are non-toxic. Kokalari et al., (2021) study reported that carbon nanoparticles do not enhance the cell viability reduction in human bronchial epithelial cells (BEAS-2B) and human lung cancer cells (A549 and NCI-H1650), and on upto 160  $\mu\text{g/mL}$ . Similarly, the Dehvari et al., (2019) study demonstrated that crab shell-derived carbon nanodots do not promote cell death up to 1000  $\mu\text{g/mL}$ . In addition, a previous study reported that Palmyra palm leaf-derived carbon dots did not affect cell viability even at 400  $\mu\text{g/mL}$  concentration

(Athinarayanan et al., 2020a). Furthermore, we have investigated the cell uptake through bright-field microscopy. We found that the CCNs and CCNs/PA accumulates in macrophages (Fig. 7). The black accumulation was observed intracellularly based on the dose range. These results attributed the cellular uptake of CCNs/PA and did not promote any adverse changes in cell structure. This result inferred that the size of the particles correlates with more intracellular uptake on CCNs/PA, which is constant with the examination in THP-1 macrophages. The intracellular localization of CCNs and CCNs/PA were revealed using bright-field microscopic images. Nuclear morphological modulations of cells are vital for identifying apoptotic cell death. After exposure to CCNs and CCNs/PA for 24 h, nuclear morphological changes were observed in CCNs-treated cells (Fig. 7a). CCNs induce apoptotic cell death in THP-1 macrophages, but cells treated with CCNs/PA remained healthy, with no changes seen (Fig. 7b). Fig. 8 shows the Wright-Giemsa staining of CCNs/PA-treated macrophages. We examined the CNs decorated PA aggregates as black bunch-like structures in CCNs/PA treated macrophages. But no modulation in intracellular structures. Our results suggested that CCNs/PA do not cause cell death or any cellular structure modulations. It inferred that CCNs/PA are non-toxic in macrophages. Hence, these nanostructures can be used in biological applications. Oil-red O staining results are shown in Fig. 9. It shows

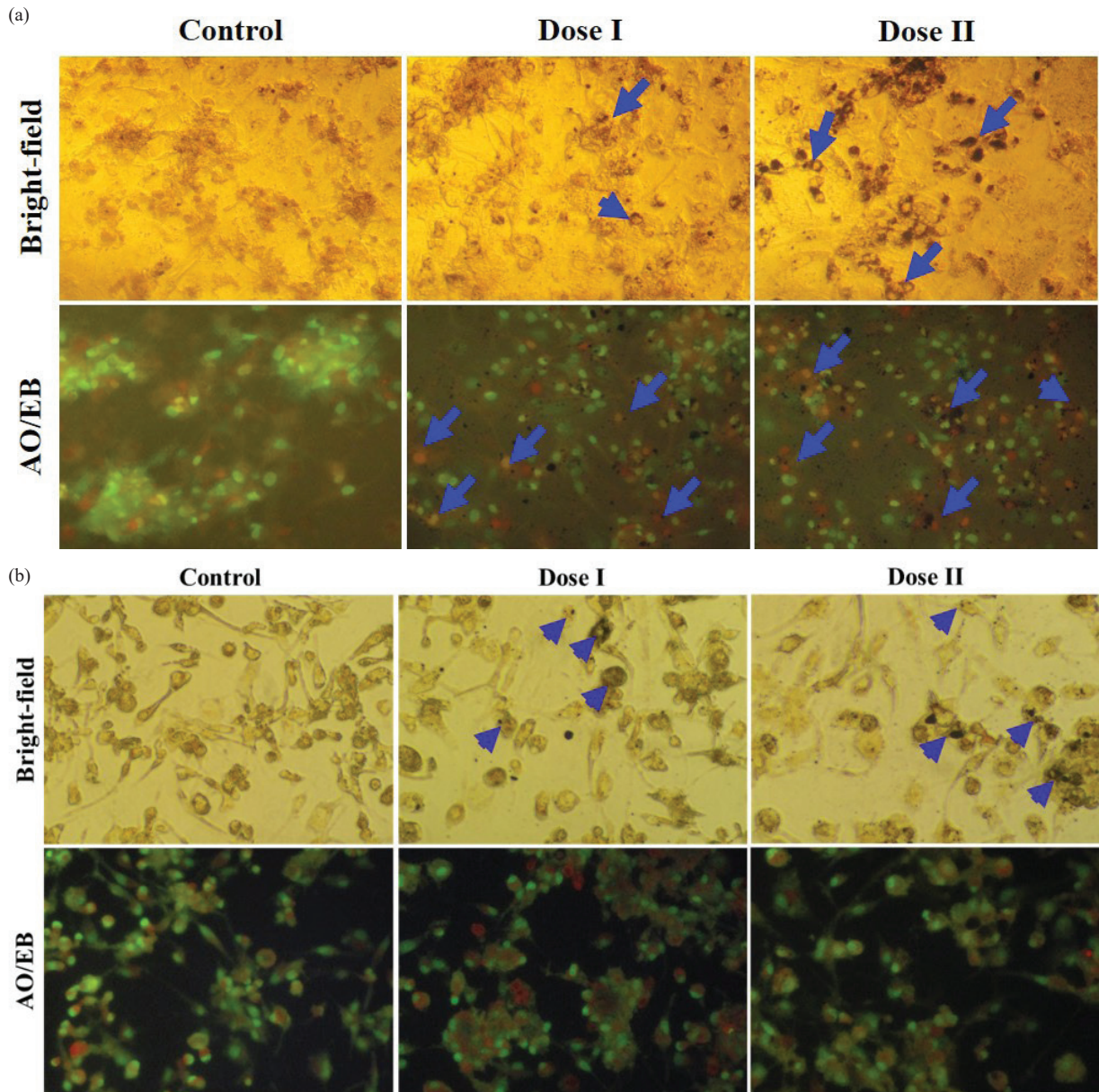


**Fig. 7.** (a) Morphological features of THP-1 macrophages without and with exposure to CCNs. After THP-1 cells differentiate into macrophages using PMA and are exposed to CCNs, Control = 0  $\mu\text{g/mL}$ , Dose I = 50  $\mu\text{g/mL}$ ; Dose II = 100  $\mu\text{g/mL}$  for 24 h. Images were captured using bright-field microscopy at 400x. A blue arrow indicates an accumulation of CCNs. Nuclear morphological changes of THP-1 macrophages without and with exposure to CCNs (Control, Dose I = 50  $\mu\text{g/mL}$ ; Dose II = 100  $\mu\text{g/mL}$ ) for 24 h. The cells were stained with AO/EB, and images were captured using fluorescence microscopy at 400X. (b) Morphological features of THP-1 macrophages without and with exposure to CCNs/PA. After THP-1 cells differentiate into macrophages using PMA and are exposed to CCNs/PA, Control = 0  $\mu\text{g/mL}$ , Dose I = 50  $\mu\text{g/mL}$ ; Dose II = 100  $\mu\text{g/mL}$  for 24 h. Images were captured using bright-field microscopy at 400x. A blue arrow indicates an accumulation of CCNs/PA. Nuclear morphological changes of THP-1 macrophages without and with exposure to CCNs/PA. After THP-1 cells differentiate into macrophages using PMA and are exposed to CCNs/PA (Control, Dose I = 50  $\mu\text{g/mL}$ ; Dose II = 100  $\mu\text{g/mL}$ ) for 24 h. The cells were stained with AO/EB, and images were captured using fluorescence microscopy at 400X.

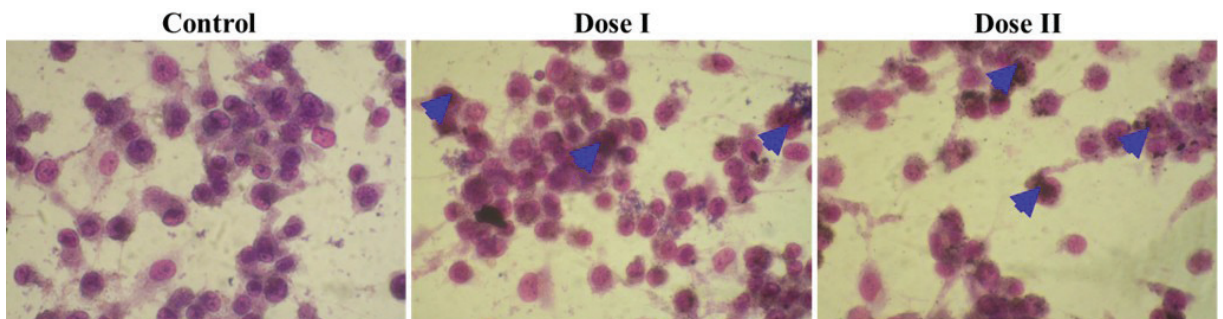


**Fig. 8.** Effects of CCNs/PA on morphological changes in THP-1 macrophages. Following 24 h of CCNs/PA treatment, irregular changes in morphology were detected when compared with the control. Control = 0  $\mu\text{g/mL}$ , Dose I = 50  $\mu\text{g/mL}$ ; Dose II = 100  $\mu\text{g/mL}$  for 24 h. The cells were stained with Giemsa, and images were captured using light microscopy at 400X. A blue arrow indicates an accumulation of CCNs/PA.

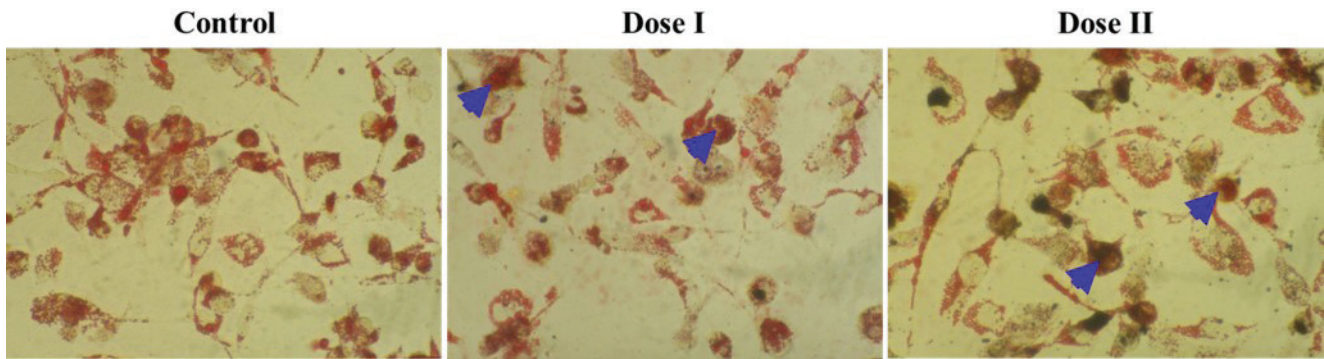


**Fig. 9.** Effects of CCNs/PA on cellular uptake in THP-1 macrophages. Cell structural features of THP-1 macrophages without and with exposure to CCNs/PA. Control = 0  $\mu\text{g/mL}$ ; Dose I = 50  $\mu\text{g/mL}$ ; Dose II = 100  $\mu\text{g/mL}$  for 24 h. The cells were stained with Oil Red O stain, and images were captured using light microscopy at 400X. A blue arrow indicates lipid droplet accumulation.

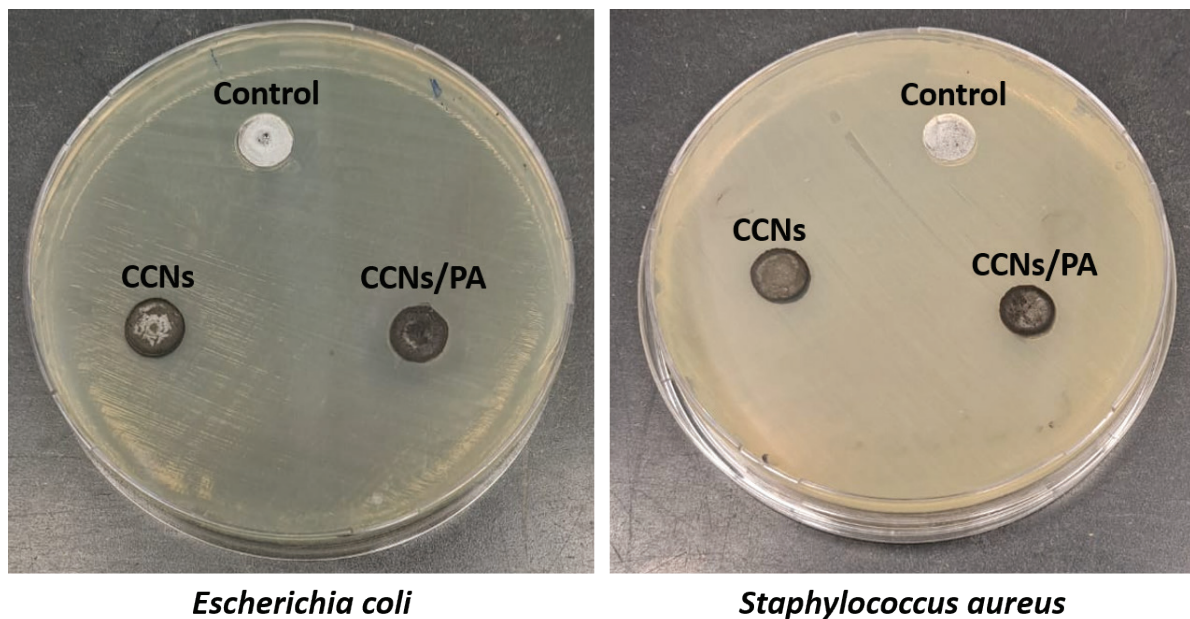


**Fig. 10.** Antimicrobial activity of CCNs and CCNs/PA.

the CNs attached to PA presence in macrophages. The dark red spherule-like structures found in CCNs/PA treated cells. Our results suggest that CCNs/PA exhibited no significant cytotoxic effects in macrophages. We have assessed the antibacterial potential of CCNs and CCNs/PA, shown in Fig. 10. The CCNs lack antibacterial activity against *E. coli* and *Staphylococcus aureus*. The PA -decorated carbon nanoparticles exhibited an antibacterial effect on *E. coli* but not on *Staphylococcus aureus* (Table S1). Our results clearly indicate that CCNs/PA exhibit antibacterial activity due to the presence of PA.

#### 4. Conclusions

We have synthesized edible oil-derived CNs with a range of particle sizes between 70 – 100 nm. The CCNs were analyzed using different techniques, including TEM, XRD, XPS, and FTIR. XPS analysis of CNs displays typical peaks at 284.2 and 532.8 eV, attributed to C1s and O1s, respectively. The CCNs surface was modified with PA, and the cytotoxicity and cellular uptake in THP-1-derived macrophages were evaluated. An *in vitro* cytotoxicity results indicated that CCNs/PA do not alter the viability of macrophages due to their good compatibility. Also, these materials do not modulate cellular morphological changes in macrophages. These results suggest no significant difference between CCNs/PA cytotoxic features was observed. In summary, the prepared CCNs/PA may be applied in biomedical applications for further investigation.

#### CRediT authorship contribution statement

**Abdullah Almubarak:** Methodology, investigation, formal analysis, writing – original draft preparation; **Vaiyapuri Subbarayan Periasamy:** Conceptualization, methodology, investigation; **Jegan Athinarayanan:** Methodology, investigation, formal analysis; **Ali A Alshatwi:** Conceptualization, resources, writing – review & editing.

#### Declaration of competing interest

The authors declare that they have no known competing financial interests or personal relationships that could have appeared to influence the work reported in this paper

#### Data availability

The original contributions presented in this study are included in the article/supplementary material. Further inquiries can be directed to the corresponding author(s).

#### Declaration of generative AI and AI-assisted technologies in the writing process

The authors confirm that there was no use of artificial intelligence (AI)-assisted technology for assisting in the writing or editing of the manuscript and no images were manipulated using AI.

## Acknowledgment

The authors would like to extend their gratitude to the Ongoing Research Funding Program (ORF-2026-178), King Saud University, Riyadh, Saudi Arabia for providing financial, technical and administrative support.

## Funding:

Ongoing Research Funding program (ORF-2026-178), King Saud University, Riyadh, Saudi Arabia.

## Supplementary data

Supplementary material to this article can be found online at [https://dx.doi.org/10.25259/JKSUS\\_1824\\_2025](https://dx.doi.org/10.25259/JKSUS_1824_2025).

## References

- Alsaffar, R., Al-Dabbagh, B., Jawad, H., 2023. Preparation of black carbon nanoparticles from two sources of oil residues with direct and indirect ultrasonic process. *JASN* 3, 10-19. <https://doi.org/10.53293/jasn.2023.6760.1207>
- Arroyo-Arroyo, C., Granados-Martinez, F.G., Domratcheva-Lvova, L., Hernandez-Cristóbal, O., Flores-Ramirez, N., Vásquez-García, S., 2024. Synthesis and functionalization of carbon nanostructures in a single-step CVD process through the implementation of a recycled precursor. *J of Chemical Tech & Biotech* 99, 2503-2508. <https://doi.org/10.1002/jctb.7604>
- Atchudan, R., Edison, T.N.J.I., Perumal, S., Muthuchamy, N., Lee, Y.R., 2020. Hydrophilic nitrogen-doped carbon dots from biowaste using dwarf banana peel for environmental and biological applications. *Fuel* 275, 117821. <https://doi.org/10.1016/j.fuel.2020.117821>
- Athinarayanan, J., Periasamy, V.S., Alatiyah, K.A., Alshatwi, A.A., 2020. Synthesis and cytocompatibility analysis of carbon nanodots derived from palmyra palm leaf for multicolor imaging applications. *Sustain Chem Pharm* 18, 100334. <https://doi.org/10.1016/j.scp.2020.100334>
- Athinarayanan, J., Periasamy, V.S., Alshatwi, A.A., 2025. Carbon quantum dots in palmyra palm jaggery: Evaluation of antioxidative and cytocompatibility features. *Sugar Tech* 27, 367-377. <https://doi.org/10.1007/s12355-024-01504-y>
- Athinarayanan, J., Periasamy, V.S., Alshatwi, A.A., 2018. Fabrication and cytotoxicity assessment of cellulose nanofibrils using *Bassia eriophora* biomass. *Int J Biol Macromol* 117, 911-918. <https://doi.org/10.1016/j.ijbiomac.2018.05.144>
- Athinarayanan, J., Periasamy, V.S., Alshatwi, A.A., 2024. Isolation of nanostructured carbon particles from sugarcane jaggery: Evaluation of their antioxidant and cytotoxic features. *Diam Relat Mater* 149, 111522. <https://doi.org/10.1016/j.diamond.2024.111522>
- Athinarayanan, J., Periasamy, V.S., Alshatwi, A.A., 2020. Simultaneous fabrication of carbon nanodots and hydroxyapatite nanoparticles from fish scale for biomedical applications. *Mater Sci Eng C Mater Biol Appl* 117, 111313. <https://doi.org/10.1016/j.msec.2020.111313>
- Athinarayanan, J., Periasamy, V.S., Alshatwi, A.A., 2022. Unveiling the biocompatible properties of date palm tree (*Phoenix dactylifera* L.) biomass-derived lignin nanoparticles. *ACS Omega* 7, 19270-19279. <https://doi.org/10.1021/acsomega.2c00753>
- Bagheri, B., Surwase, S.S., Lee, S.S., Park, H., Faraji Rad, Z., Trevaskis, N.L., Kim, Y.C., 2022. Carbon-based nanostructures for cancer therapy and drug delivery applications. *J Mater Chem B* 10, 9944-9967. <https://doi.org/10.1039/d2tb01741e>
- Cao, Y., Roursgaard, M., Danielsen, P.H., Møller, P., Loft, S., 2014. Carbon black nanoparticles promote endothelial activation and lipid accumulation in macrophages independently of intracellular ROS production. *PLoS One* 9, e106711. <https://doi.org/10.1371/journal.pone.0106711>
- Carta, G., Murru, E., Banni, S., Manca, C., 2017. Palmitic acid: Physiological role, metabolism and nutritional implications. *Front Physiol* 8, 902. <https://doi.org/10.3389/fphys.2017.00902>
- Chang, B.P., Gupta, A., Mekonnen, T.H., 2021. Flame synthesis of carbon nanoparticles from corn oil as a highly effective cationic dye adsorbent. *Chemosphere* 282, 131062. <https://doi.org/10.1016/j.chemosphere.2021.131062>
- Clancy, A.J., Bayazit, M.K., Hodge, S.A., Skipper, N.T., Howard, C.A., Shaffer, M.S.P., 2018. Charged carbon nanomaterials: Redox chemistries of fullerenes, carbon nanotubes, and graphenes. *Chem Rev* 118, 7363-7408. <https://doi.org/10.1021/acs.chemrev.8b00128>
- Dehvari, K., Liu, K.Y., Tseng, P.J., Gedda, G., Girma, W.M., Chang, J.Y., 2019. Sonochemical-assisted green synthesis of nitrogen-doped carbon dots from crab shell as targeted nanoprobes for cell imaging. *J Taiwan Inst Chem Eng* 95, 495-503. <https://doi.org/10.1016/j.jtice.2018.08.037>
- Erbay, E., Babaev, V.R., Mayers, J.R., Makowski, L., Charles, K.N., Snitow, M.E., Fazio, S., Wiest, M.M., Watkins, S.M., Linton, M.F., Hotamisligil, G.S., 2009. Reducing endoplasmic reticulum stress through a macrophage lipid chaperone alleviates atherosclerosis. *Nat Med* 15, 1383-1391. <https://doi.org/10.1038/nm.2067>
- Feng, Y., Lu, S., Zhao, Q., Sun, T., Shi, Y., Gao, G., Wang, H., Zhi, J., 2024. Controlled phase transition of the onion-like carbon nanostructure for photothermal cancer therapy. *ACS Appl Nano Mater* 7, 7008-7017. <https://doi.org/10.1021/acsnano.3c06107>
- Georgakilas, V., Perman, J.A., Tucek, J., Zboril, R., 2015. Broad family of carbon nanoallotropes: Classification, chemistry, and applications of fullerenes, carbon dots, nanotubes, graphene, nanodiamonds, and combined superstructures. *Chem Rev* 115, 4744-4822. <https://doi.org/10.1021/cr500304f>
- Germic, N., Frangez, Z., Yousefi, S., Simon, H.U., 2019. Regulation of the innate immune system by autophagy: Monocytes, macrophages, dendritic cells and antigen presentation. *Cell Death Differ* 26, 715-727. <https://doi.org/10.1038/s41418-019-0297-6>
- Gusain, R., Kumar, N., Ray, S.S., 2020. Recent advances in carbon nanomaterial-based adsorbents for water purification. *Coord Chem Rev* 405, 213111. <https://doi.org/10.1016/j.ccr.2019.213111>
- Habelreth, H.H., Athinarayanan, J., Periasamy, V.S., Alshatwi, A.A., 2025. Antioxidant activity and immunocompatibility of maillared carbon dots derived from arginine-glucose model system. *Food Biosci* 64, 105916. <https://doi.org/10.1016/j.fbio.2025.105916>
- Kaare, K., Volperts, A., Plavnicec, A., Walke, P., Kämbre, T., Noor, N., Foroozan, A., Higgins, D.C., Praats, R., Liivand, K., Tamasauskaitė-Tamasiunaite, L., Colmenares-Rausseo, L., Lilloja, J., Tammeveski, K., Krusenbergs, I., 2024. Heteroatom-doped carbon nanomaterials derived from black liquor for electrochemical oxygen reduction reaction. *ACS Sustainable Resour Manage* 1, 1705-1716. <https://doi.org/10.1021/acssusresmt.4c00022>
- Kanakaraj, R., Sudakar, C., 2020. Candle soot carbon nanoparticles as high-performance universal anode for M-ion (M = Li+, Na+ and K+) batteries. *J Power Sources* 458, 228064. <https://doi.org/10.1016/j.jpowsour.2020.228064>
- Kinaret, P.A.S., Scala, G., Federico, A., Sund, J., Greco, D., 2020. Carbon nanomaterials promote M1/M2 macrophage activation. *Small* 16, e1907609. <https://doi.org/10.1002/smll.201907609>
- Kokalari, I., Keshavan, S., Rahman, M., Gazzano, E., Barzan, G., Mandrile, L., Giovannozzi, A., Ponti, J., Antonello, G., Monopoli, M., Perrone, G., Bergamaschi, E., Riganti, C., Fadeel, B., Fenoglio, I., 2021. Efficacy, biocompatibility and degradability of carbon nanoparticles for photothermal therapy of lung cancer. *Nanomedicine (Lond)* 16, 689-707. <https://doi.org/10.2217/nmm-2021-0009>
- Korbecki, J., Bajdak-Rusinek, K., 2019. The effect of palmitic acid on inflammatory response in macrophages: An overview of molecular mechanisms. *Inflamm Res* 68, 915-932. <https://doi.org/10.1007/s00011-019-01273-5>
- Long, J., Ma, W., Yu, Z., Liu, H., Cao, Y., 2019. Multi-walled carbon nanotubes (MWCNTs) promoted lipid accumulation in THP-1 macrophages through modulation of endoplasmic reticulum (ER) stress. *Nanotoxicology* 13, 938-951. <https://doi.org/10.1080/17435390.2019.1597204>
- Malode, S.J., Pandiaraj, S., Alodhayb, A., Shetti, N.P., 2024. Carbon nanomaterials for biomedical applications: Progress and outlook. *ACS Appl Bio Mater* 7, 752-777. <https://doi.org/10.1021/acsbm.3c00983>
- Mulay, M.R., Chauhan, A., Patel, S., Balakrishnan, V., Halder, A., Vaish, R., 2019. Candle soot: Journey from a pollutant to a functional material. *Carbon* 144, 684-712. <https://doi.org/10.1016/j.carbon.2018.12.083>
- Nadeem, S., Rasool, M., Javed, M., Iqbal, S., Mahmood, S., Allah Ditta, N., Mohyuddin, A., Bahadur, A., Alshatwi, M., 2024. Preparation of carbon nanoparticles constructed from seed oils, physical characterizations and antifungal performance. *Inorg Chem Commun* 159, 111774. <https://doi.org/10.1016/j.inoche.2023.111774>
- Periasamy, K., Darouie, M., Das, R., Khatibi, A.A., 2024. Investigating the potential of ghee precursor-derived carbon nano onions for enhancing interfacial bonding in thermoplastic composites. *Molecules* 29, 928. <https://doi.org/10.3390/molecules29050928>
- Phuangbubpha, P., Thara, S., Sriboonai, P., Saetan, P., Tumnoi, W., Charoenpanich, A., 2023. Optimizing THP-1 macrophage culture for an immune-responsive human intestinal model. *cells* 12, 1427. <https://doi.org/10.3390/cells12101427>
- Qin, Z., 2012. The use of THP-1 cells as a model for mimicking the function and regulation of monocytes and macrophages in the vasculature. *Atherosclerosis* 221, 2-11. <https://doi.org/10.1016/j.atherosclerosis.2011.09.003>
- Ramar, V., Balraj, A., 2022. Critical review on carbon-based nanomaterial for carbon capture: Technical challenges, opportunities, and future perspectives. *Energy Fuels* 36, 13479-13505. <https://doi.org/10.1021/acs.energyfuels.2c02585>
- Riley, P.R., Narayan, R.J., 2021. Recent advances in carbon nanomaterials for biomedical applications: A review. *Curr Opin Biomed Eng* 17, 100262. <https://doi.org/10.1016/j.cobme.2021.100262>
- Rosa Neto, J.C., Calder, P.C., Curi, R., Newsholme, P., Sethi, J.K., Silveira, L.S., 2021. The immunometabolic roles of various fatty acids in macrophages and lymphocytes. *Int J Mol Sci* 22, 8460. <https://doi.org/10.3390/ijms22168460>
- Saini, D., Gunture, Kaushik, J., Aggarwal, R., Tripathi, K.M., Sonkar, S.K., 2021. Carbon nanomaterials derived from black carbon soot: A review of materials and applications. *ACS Appl Nano Mater* 4, 12825-12844. <https://doi.org/10.1021/acsnano.1c02840>
- Shapouri-Moghaddam, A., Mohammadian, S., Vazini, H., Taghadosi, M., Esmaili, S.A., Mardani, F., Seifi, B., Mohammadi, A., Afshari, J.T., Sahebkar, A., 2018. Macrophage plasticity, polarization, and function in health and disease. *J Cell Physiol* 233, 6425-6440. <https://doi.org/10.1002/jcp.26429>
- Shen, L., Zhang, L., Chen, M., Chen, X., Wang, J., 2013. The production of pH-sensitive photoluminescent carbon nanoparticles by the carbonization of polyethylenimine and their use for bioimaging. *Carbon* 55, 343-349. <https://doi.org/10.1016/j.carbon.2012.12.074>
- Singh, V.P., Date, I.M., Sharma, J.D., 2025. A review on waste carbon soot as a functional material for water remediation. *Int J Environ Sci Technol* 22, 2793-2808. <https://doi.org/10.1007/s13762-024-05886-0>
- Tyagi, A., Mishra, K., Sharma, S.K., Shukla, V.K., 2022. Performance studies of an electric double-layer capacitor (EDLC) fabricated using edible oil-derived activated carbon. *J Mater Sci: Mater Electron* 33, 8920-8934. <https://doi.org/10.1007/s10854-021-06978-0>

- Wang, X., Lin, T., Wu, W., Wu, H., Yan, D., 2022. Synthesis of N-doped carbon dots for highly selective and sensitive detection of metronidazole in real samples and its cytotoxicity studies. *Environ Technol* 43, 4213-4226. <https://doi.org/10.1080/09593330.2021.1946164>
- Yan, Z.Q., Hansson, G.K., 2007. Innate immunity, macrophage activation, and atherosclerosis. *Immunol Rev* 219, 187-203. <https://doi.org/10.1111/j.1600-065X.2007.00554.x>
- Yang, Z., Xu, T., Li, H., She, M., Chen, J., Wang, Z., Zhang, S., Li, J., 2023. Zero-dimensional carbon nanomaterials for fluorescent sensing and imaging. *Chem Rev* 123, 11047-11136. <https://doi.org/10.1021/acs.chemrev.3c00186>
- Zhu, H., Wang, X., Li, Y., Wang, Z., Yang, F., Yang, X., 2009. Microwave synthesis of fluorescent carbon nanoparticles with electrochemiluminescence properties. *Chem Commun (Camb)* 5118-5120. <https://doi.org/10.1039/b907612c>